Supporting Information

Photoredox Catalysis Enabled by Atomically Precise Metal Nanoclusters

Junyi Zhang[a], Linjian Zhan[a], Boyuan Ning[a], Yunhui He[a,b], Guangcan Xiao[a,b], Zhixin Chen[a,b], Fang-Xing Xiao[c*]

a. School of Advanced Manufacturing, Fuzhou University, Jinjiang, 362200, PR China

b. Instrumental Measurement and Analysis Center, Fuzhou University, Fuzhou 350108, PR China

c. College of Materials Science and Engineering, Fuzhou University, Fuzhou 350108, PR China.

Email: xgc@fzu.edu.cn; fxxiao@fzu.edu.cn

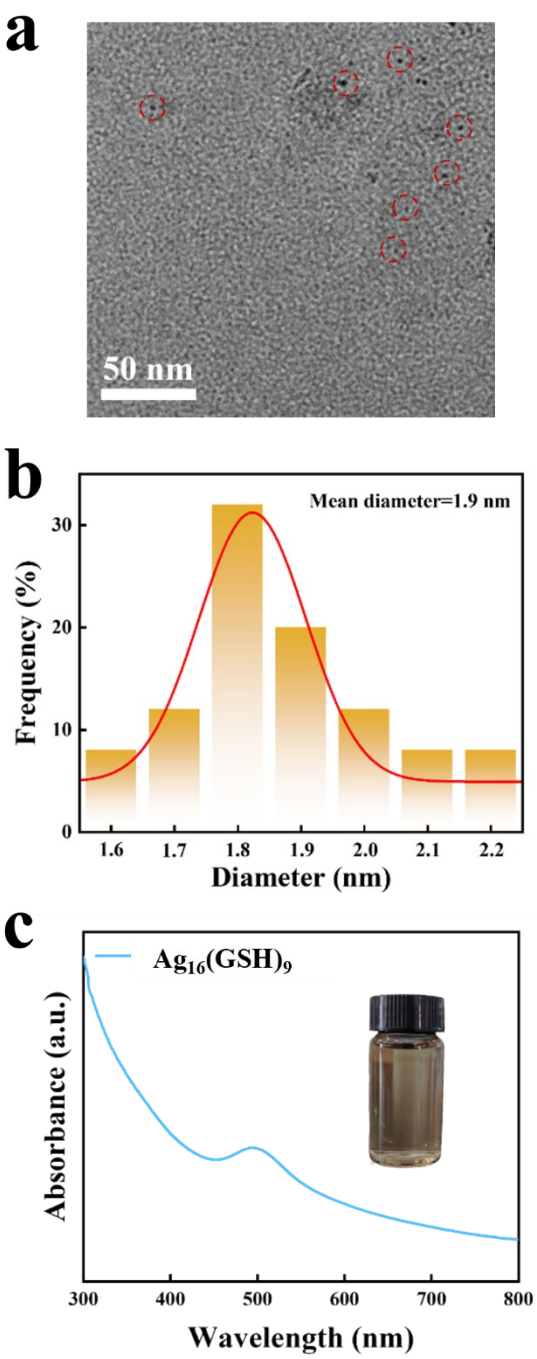

Fig. S1. (a) TEM image of $Ag_{16}(GSH)_9$ NCs with the corresponding (b) size distribution histogram and, (c) UV-vis absorption spectrum of $Ag_{16}(GSH)_9$ NCs.

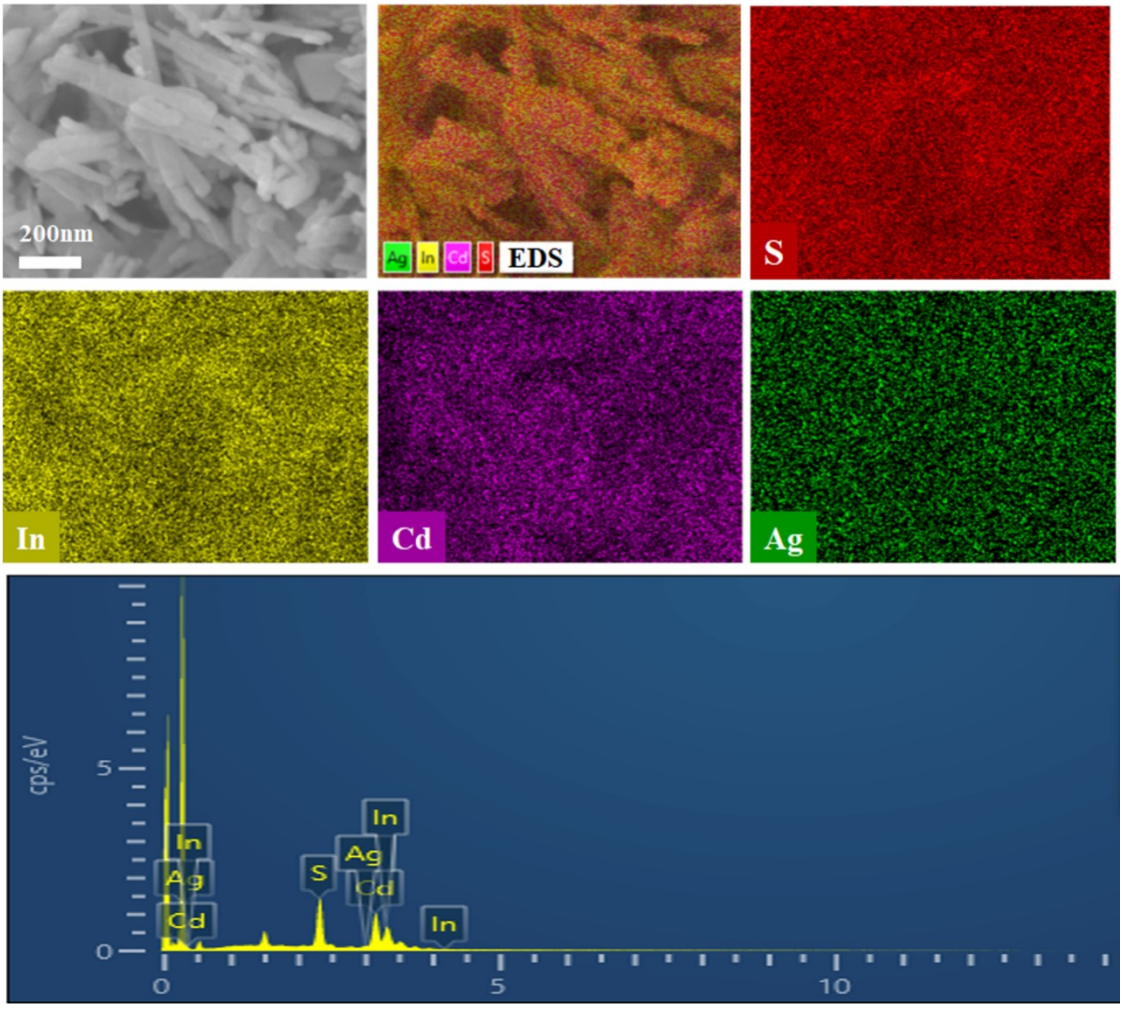

Fig. S2. FESEM image of CIS/$Ag_{16}(GSH)_9$ heterostructure and EDS result.

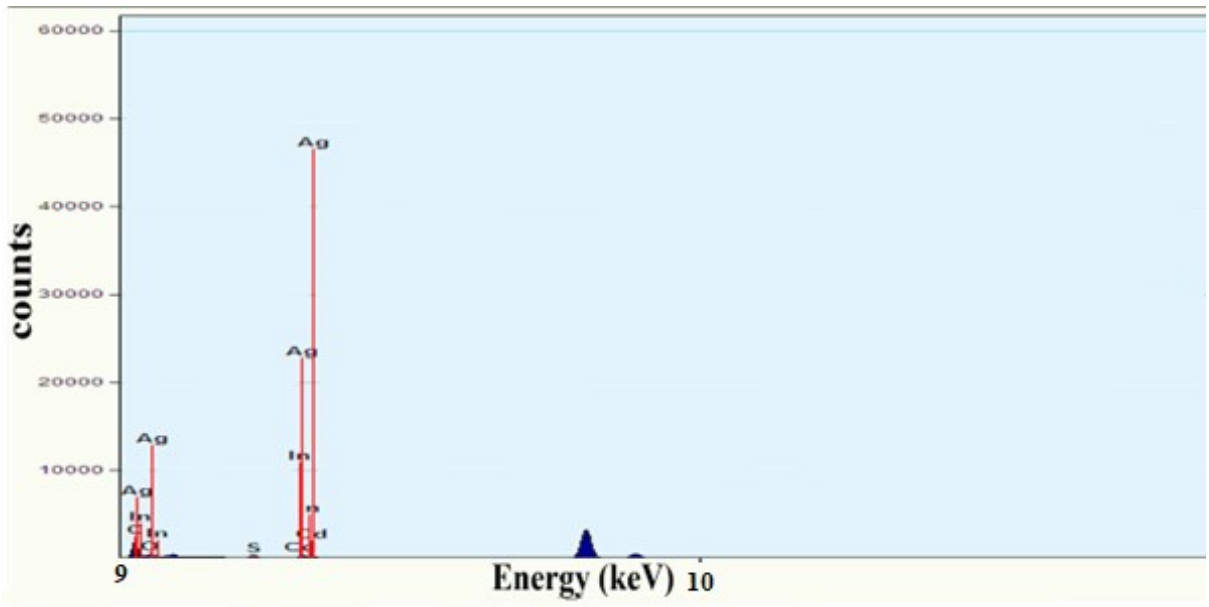

Fig S3. EDS result of CIS/$Ag_{16}(GSH)_9$ heterostructure.

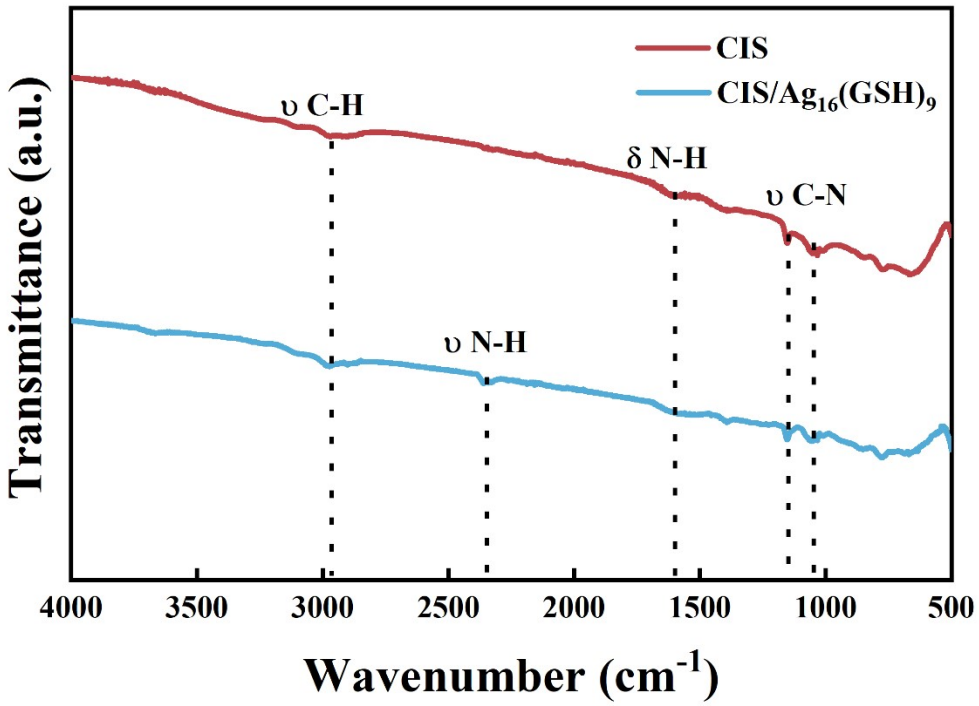

Fig S4. FTIR spectra of CIS and CIS/$Ag_{16}(GSH)_9$ heterostructure.

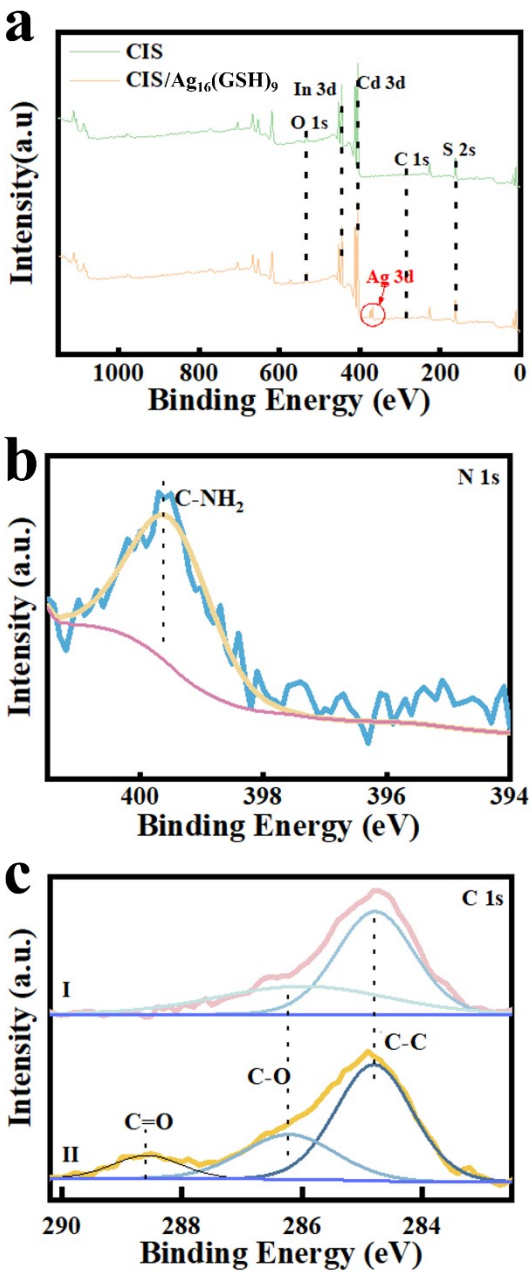

Fig. S5. (a) Survey spectra of CIS and CIS/$Ag_{16}(GSH)_9$ heterostructure, (b) high-resolution N 1s spectrum of CIS/$Ag_{16}(GSH)_9$ heterostructure and (c) high-resolution C 1s spectrum of (I) CIS and (II) CIS/$Ag_{16}(GSH)_9$ heterostructure.

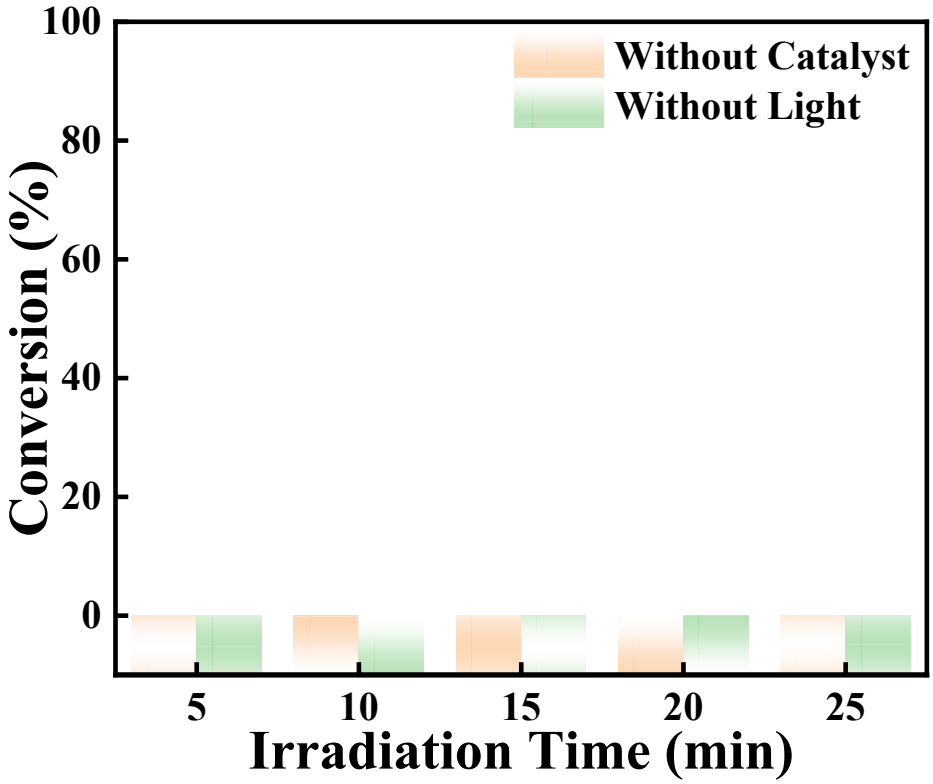

Fig. S6. Blank experiments for photocatalytic reduction of 4-NA over CIS/$Ag_{16}(GSH)_9$ heterostructure without adding catalyst and light.

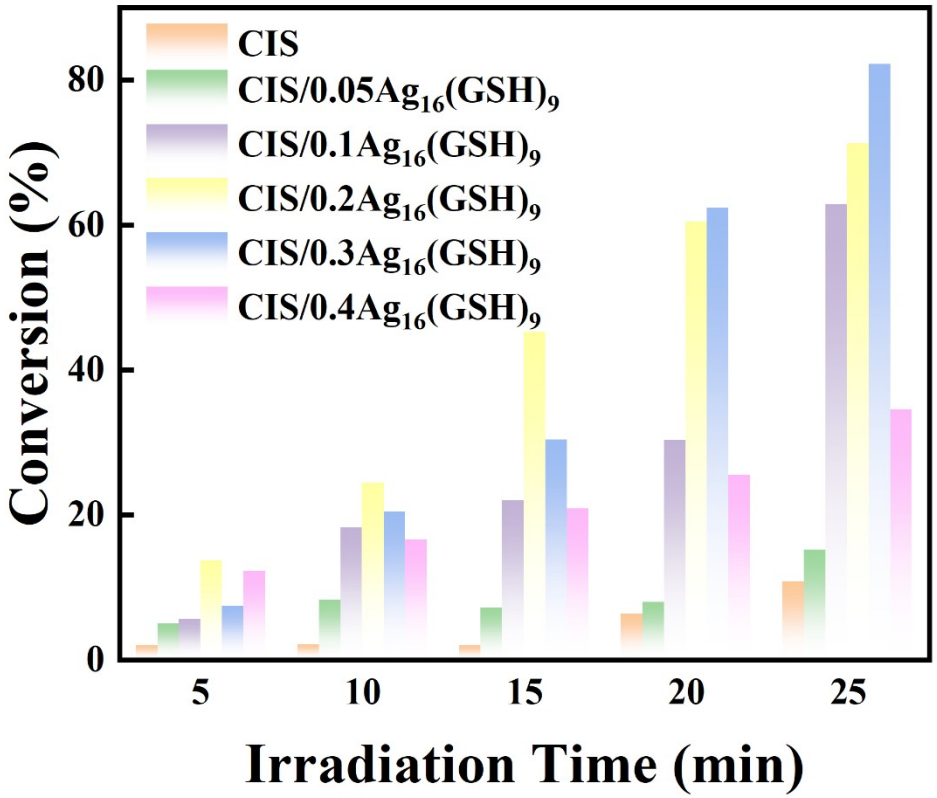

Fig. S7. Photoactivities of CIS/x$Ag_{16}(GSH)_9$ (x=0.05, 0.1, 0.2, 0.3, 0.4) heterostructure with different concentration of $Ag_{16}(GSH)_9$ NCs toward photocatalytic reduction of 4-NA under visible light irradiation ($\lambda > 420$nm).

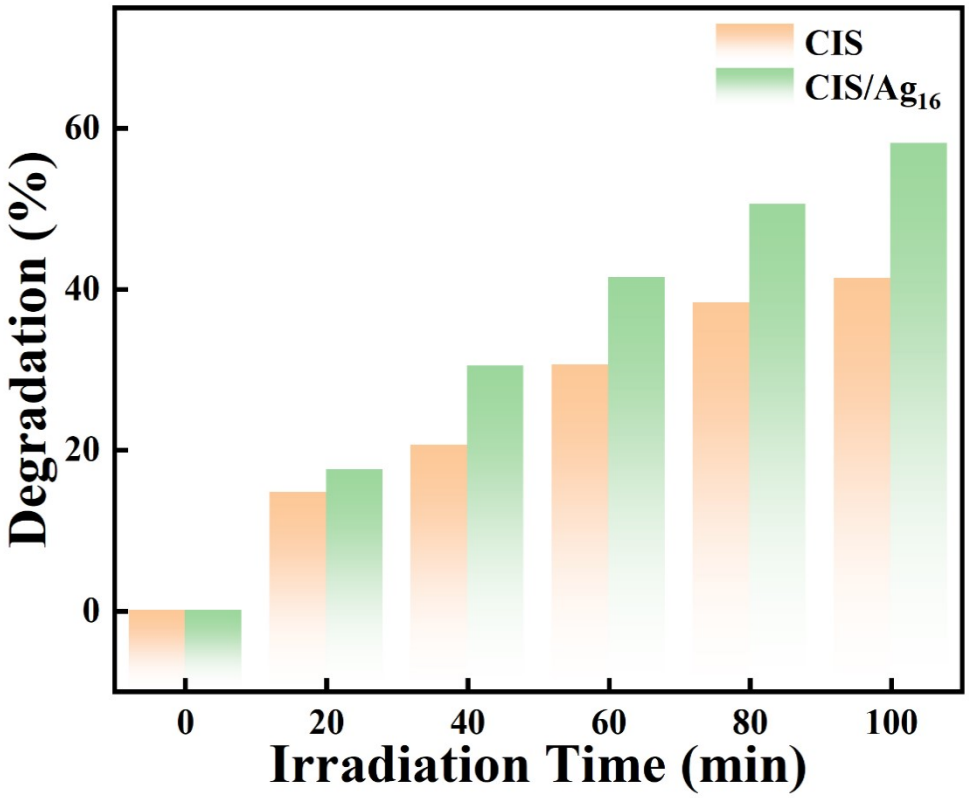

Fig. S8. Photocatalytic oxidative degradation of methyl orange by CIS and $CIS/Ag_{16}(GSH)_9$ heterostructure under visible light ($\lambda > 420$ nm).

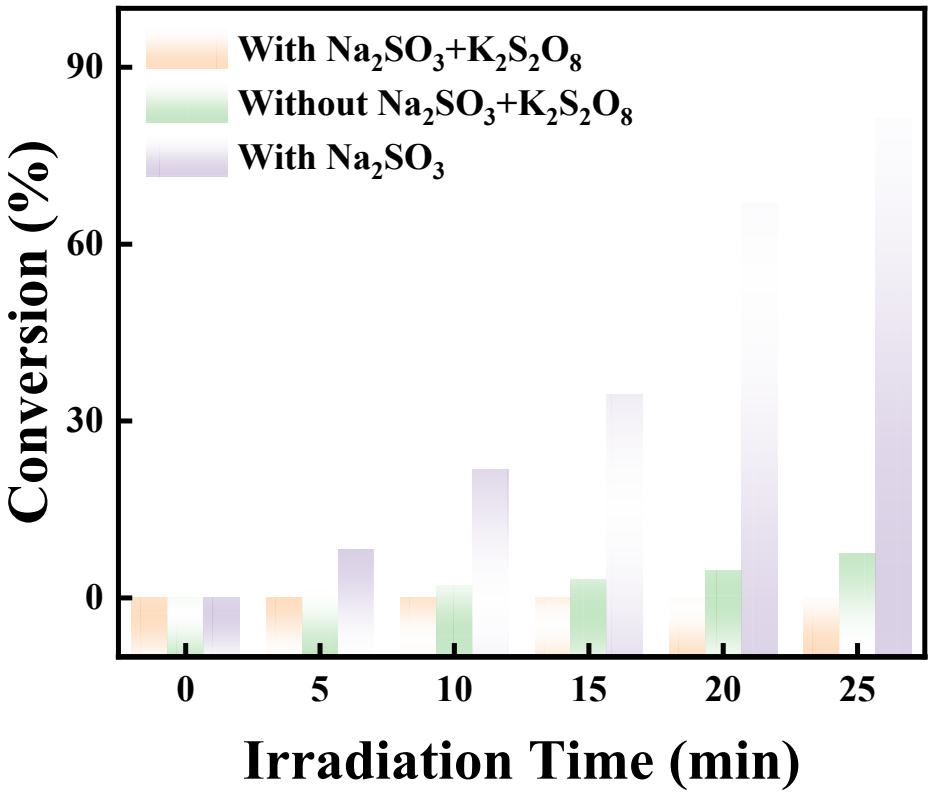

Fig. S9. Photoreduction of 4-NA over CIS/$Ag_{16}(GSH)_9$ heterostructure under different experimental conditions.

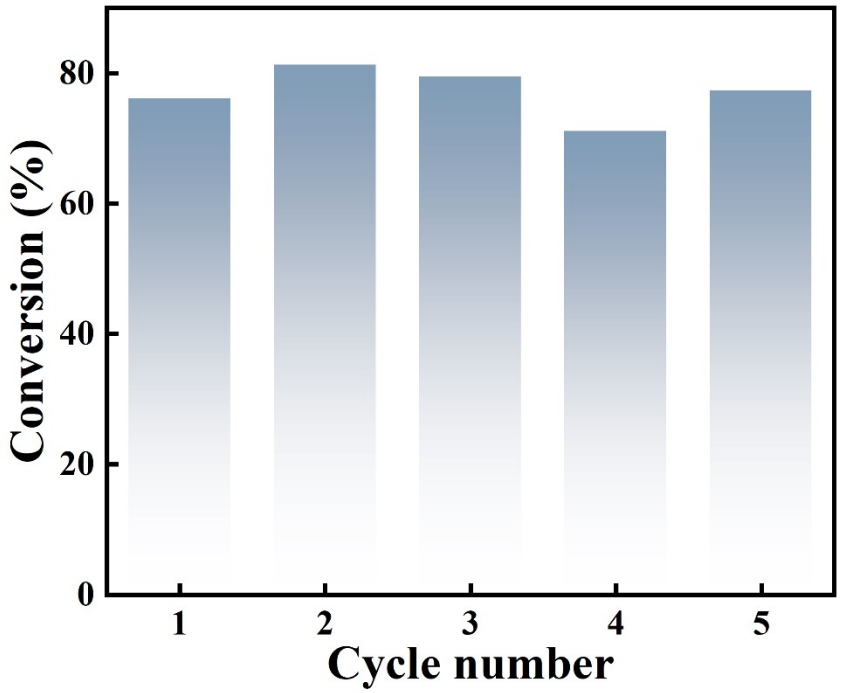

Fig. S10. Cyclic reactions of CIS/$Ag_{16}(GSH)_9$ heterostructure toward photoreduction of 4-NA.

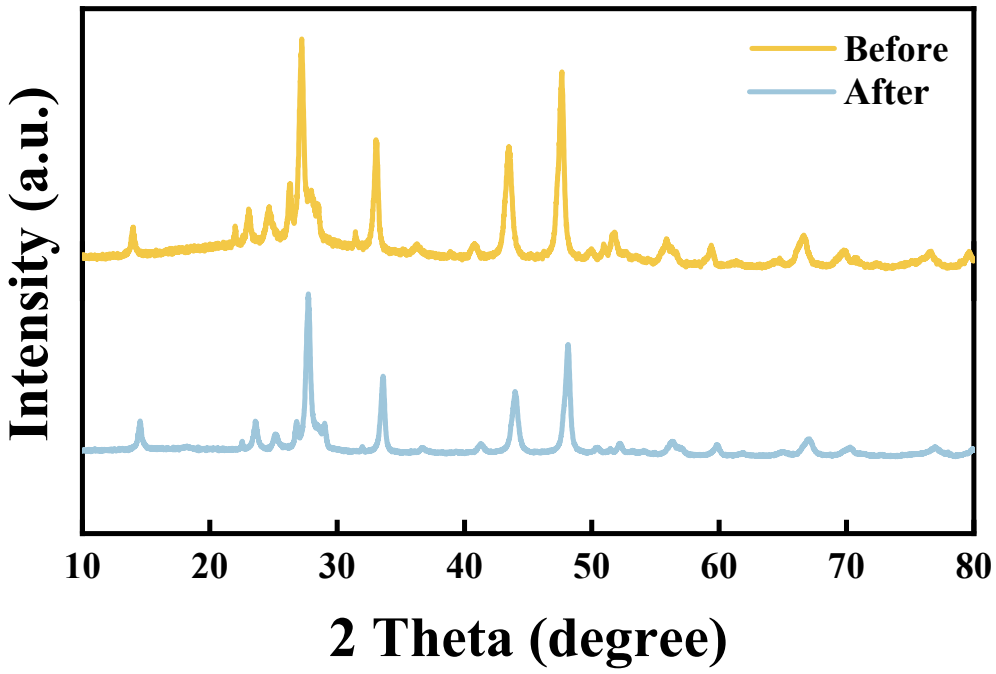

Fig. S11. XRD patterns of CIS/$Ag_{16}(GSH)_9$ heterostructure before and after 5 cyclic reactions.

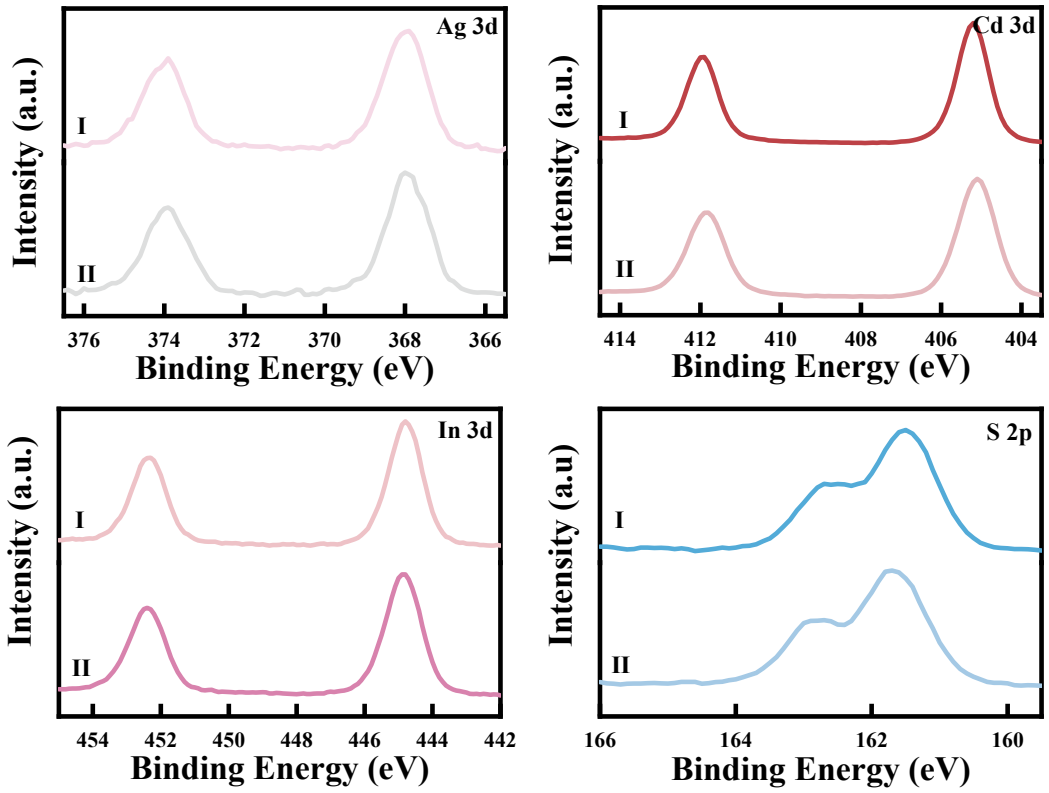

Fig. S12. High-resolution Ag 3d, Cd 3d, In 3d and S 2p spectra of CIS/$Ag_{16}(GSH)_9$

heterostructure (I) before and (II) after cyclic reactions.

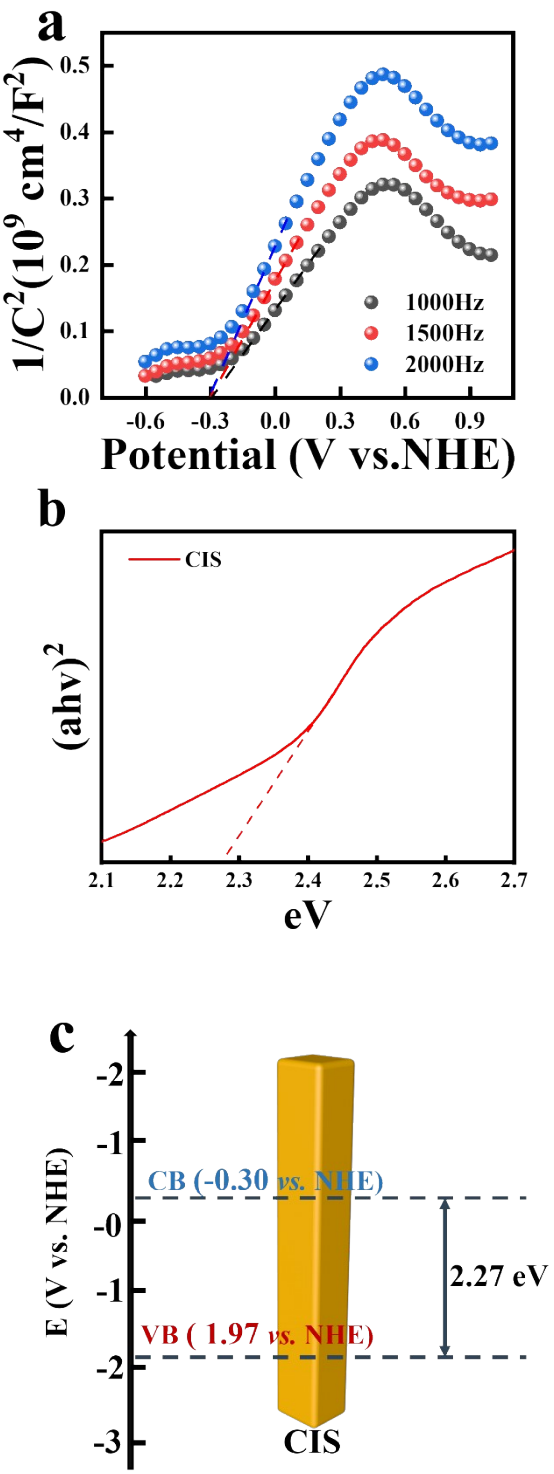

Fig. S13 (a) Mottt-Schottky plots of CIS, (b) DRS result with transformed plots based on the Kubelka-Munk function vs. the energy of light inset and (c) energy level of CIS.

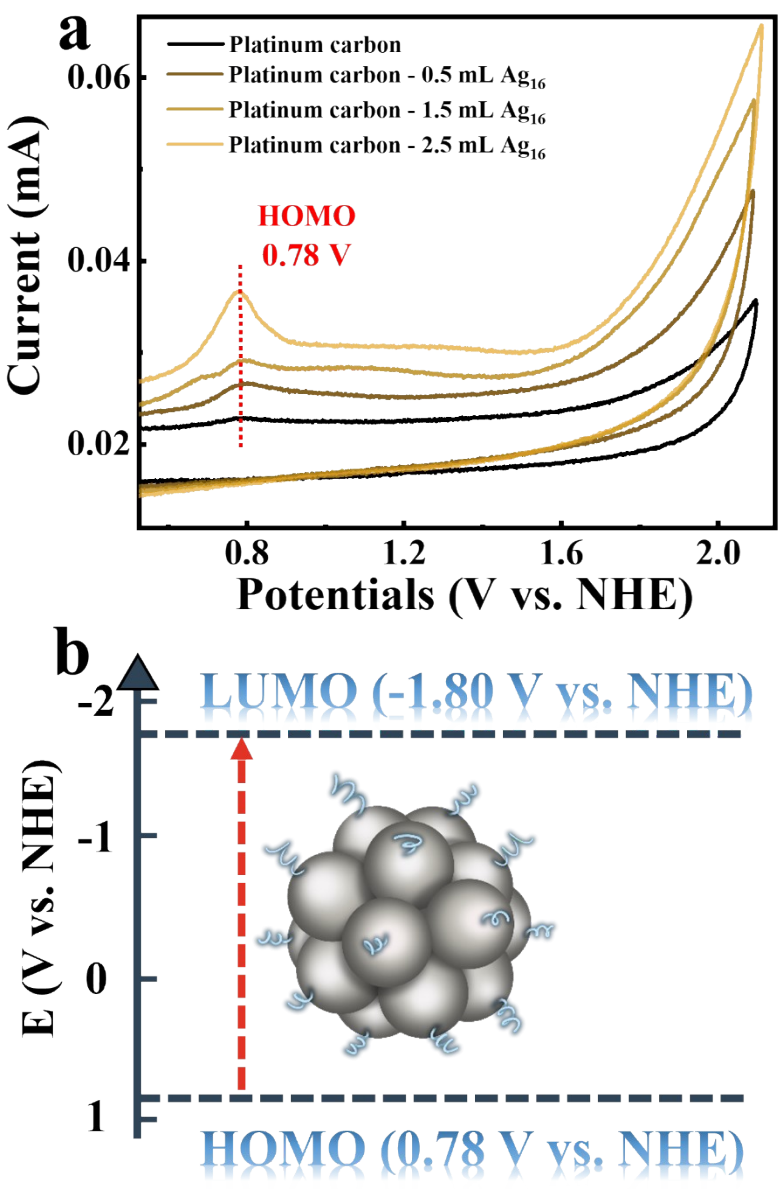

Fig. S14 (a) CV results of $Ag_{16}(GSH)_9$ NCs (electrolyte: degassed acetonitrile containing 0.1 M tetrabutyl ammonium perchlorate) and (b) energy level alignment of $Ag_{16}(GSH)_9$ NCs.

Table S1. Peak position with corresponding functional groups

Peak position (cm^{-1})	*Vibrational mode*	*Reference*
2951	υ C-H	1
1598	δ N-H	2
1142 and 1038	υ C-N	3

Table S2. Chemical bond species vs. B.E. for different samples

Elements	*CIS*	*CIS/Ag_x NCs*	*Chemical bond species*	*Reference*
C 1s	284.80	284.80	C-C	284.8 eV
S $2p_{3/2}$	161.57	161.48	S^{2-}	4
S $2p_{1/2}$	162.76	162.68	S^{2-}	4
Cd $3d_{5/2}$	405.39	405.22	Cd^{2+}	5
Cd $3d_{3/2}$	412.06	411.95	Cd^{2+}	5
In $3d_{5/2}$	444.95	444.81	In^{3+}	5
In $3d_{3/2}$	452.53	452.35	In^{3+}	5
Ag $3d_{5/2}$	None	367.82	Ag^{+}	6
Ag $3d_{5/2}$	None	368.29	Ag^{0}	7
Ag $3d_{3/2}$	None	373.79	Ag^{+}	6
Ag $3d_{3/2}$	None	374.34	Ag^{0}	7

Table S3. Specific surface area, pore volume and pore size of CIS and $CIS/Ag_{16}(GSH)_9$ heterostructure.

Samples	S_{BET} $(m^2g^{-1})^a$	Total pore volume $(cm^3g^{-1})^b$	Average pore size $(nm)^c$
CIS	15.6227	0.0699	17.897
CIS/Ag_{16}	15.0465	0.0772	20.523

a. BET surface area is calculated from the linear part of BET plots.

b. Single point total pore volume of the pores at P/P_0=0.990.

c. Adsorption average pore width (4V/A by BET)

References

1. Q. Mo, X. Lin, Z. Wei, X. Dai, S. Hou, T. Li and F. Xiao, *J. Mater. Chem. A*, 2020, **8**, 16392-16404.
2. Z. Zeng, T. Li, Y. Li, X. Dai, M. Huang, Y. He, G. Xiao and F. Xiao, *J. Mater. Chem. A*, 2018, **6**, 24686-24692.
3. Q. Zhang, Q. An, X. Luan, H. Huang, X. Li, Z. Meng, W. Tong, X. Chen, P. K. Chu and Y. Zhang, *Nanoscale*, 2015, **7**, 14002-14009.
4. Y. Song, Y. Wu, S. Cao, Y. Zhang, D. Luo, J. Gao, Z. Li, L. Sun and J. Hou, *Adv. Energy Mater.*, 2022, **12**, 2201782.
5. F. Wang, W. Zhang, H. Liu, R. Cao and M. Chen, *Chemosphere*, 2023, **338**, 139574.
6. S. W. Gaarenstroom and N. Winograd, *J. Chem. Phys.*, 1977, **67**, 3500-3506.
7. M. T. Anthony and M. P. Seah, *Surf. Interface Anal.*, 1984, **6**, 95-106.